Direct probe of the intrinsic charm content of the proton

Tom Boettcher, Philip Ilten, and Mike Williams

Phys. Rev. D **93**, 074008 — Published 7 April 2016

DOI: 10.1103/PhysRevD.93.074008

A direct probe of the intrinsic charm content of the proton

Tom Boettcher,* Philip Ilten,† and Mike Williams‡
Laboratory for Nuclear Science, Massachusetts Institute of Technology, Cambridge, MA 02139, U.S.A.

Measurement of Z bosons produced in association with charm jets (Zc) in proton-proton collisions in the forward region provides a direct probe of a potential non-perturbative (intrinsic) charm component in the proton wave function. We provide a detailed study of the potential to measure Zc production at the LHCb experiment in Runs 2 and 3 of the LHC. The sensitivity to valence-like (sea-like) intrinsic charm is predicted to be $\langle x\rangle_{\rm IC} \gtrsim 0.3\%(1\%)$. The impact of intrinsic charm on Higgs production at the LHC, including Hc, is also discussed in detail.

I. INTRODUCTION

Whether the proton wave function contains an intrinsic charm (IC) component is a topic of considerable interest (see Ref. [1] for a review). In the absence of IC, the charm (c) parton distribution function (PDF) arises entirely due to perturbative gluon radiation; however, a $|uudc\bar{c}\rangle$ component to the proton wave function is also possible. There is substantial theoretical interest in the role that non-perturbative dynamics play in the nucleon sea [2–4]. Furthermore, the presence of IC in the proton would affect the cross sections of many processes at the LHC either directly, from c or $\bar{c}$ initiated production; or indirectly, since altering the c PDF would affect other PDFs via the momentum sum rule. For example, Higgs boson production could be affected by a few percent, largely due to changes in the gluon PDF. The cross sections relevant for direct dark matter detection are sensitive to IC if the interaction is mediated by the Higgs boson [5]. IC would also affect both the rate and kinematical properties of c-hadrons produced by cosmic-ray proton interactions in the atmosphere. Semileptonic decays of such c-hadrons provide an important background to astrophysical neutrinos [6, 7].

A number of studies have been performed to determine if – and at what level – IC exists in the proton. Measurements of c-hadron production from deep inelastic scattering (DIS) [8], where the typical momentum transfer is $Q \approx 1 - 10\,\text{GeV}$, have been interpreted as evidence for percent-level c-content in the proton at large momentum fraction (x) [9–11]. If the c PDF is entirely perturbative in nature, much smaller c content at large x is expected; whereas, valence-like charm content in the proton could explain the DIS results. However, global PDF analyses tend to either provide inconclusive results on IC [12], or claim that IC is excluded at a level significantly less than 1% [13]. There is tension between some data sets applicable to such analyses where they overlap kinematically. This has led to global PDF fitters choosing either which data sets to consider, or how to handle the inherent tension between data sets in their studies. Low-energy fixed-target experiments are in principle sensitive to large-x IC, but inclusion of such low-Q data requires careful treatment of hadronic and nuclear effects. Therefore, many authors have chosen to exclude these data. Such choices inevitably affect the conclusions drawn about IC. To date, a consensus has not been reached on whether IC exists at the percent level [14, 15].

The ideal probe of IC is a high-precision measurement of an observable with direct sensitivity to the large-x charm PDF, where Q is large enough such that hadronic and nuclear effects are negligible. Measurement of the fraction of Z+jet events where the jet originates from a c quark, $Z_j^c \equiv \sigma(Zc)/\sigma(Zj)$, in the forward region at the LHC can provide such a probe. Production of Zc may proceed via $gc \to Zc$ (see Fig. 1); is inherently at large Q satisfying the constraints of Ref. [16] (due to the large Z mass); and at forward rapidities requires one initial parton to have large x, while the other must have smaller x (see Fig. 2). Differential measurement of Z_j^c provides direct sensitivity to the process $gc \to Zc$ for large-x c. The ratio Z_j^c is chosen because it is less sensitive to experimental and theoretical uncertainties than $\sigma(Zc)$.

In this article, we propose a differential measurement of Zc production in proton-proton (pp) collisions in the forward region. We show that using data that will be collected in Runs 2 and 3 of the LHC, the LHCb experiment will be highly sensitive to both valence-like and sea-like IC. While measurement of $\sigma(Zc)$ in the central region has previously been proposed to study IC [12], we will show that the impact of IC is larger in the forward region and that the LHCb detector is best suited to making a precise measurement of $\sigma(Zc)$. Finally, even in the absence of discovery of IC content in the proton, this measurement will provide a useful test of DGLAP evolution for c quarks from low-Q DIS measurements up to the electroweak scale.

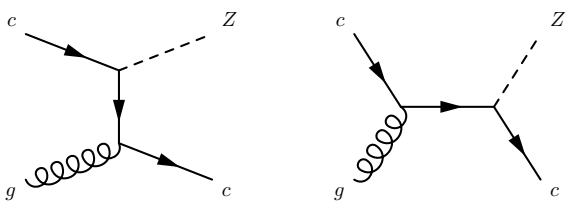

FIG. 1. Leading-order Feynman diagrams for $gc \to Zc$.

* tboettch@mit.edu
† philten@cern.ch
‡ mwill@mit.edu

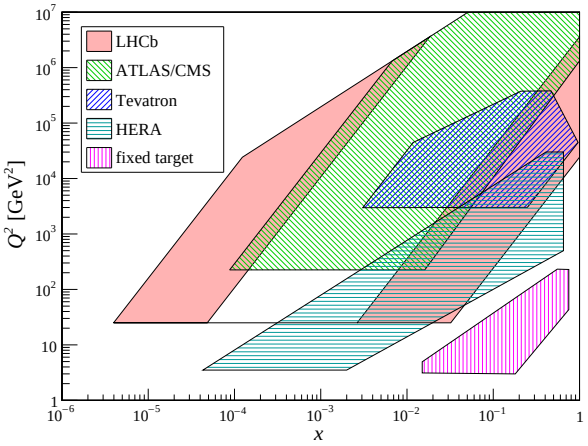

FIG. 2. Regions covered in (Q^2, x) of various experiments.

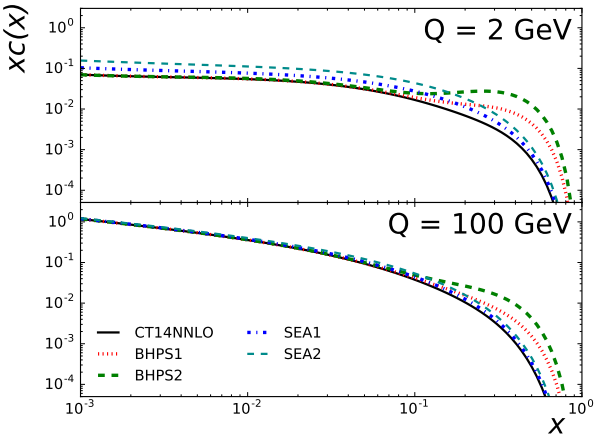

FIG. 3. IC PDFs considered [12] shown at low and high Q.

valence-like model	$\langle x\rangle_{\rm IC}$	sea-like model	$\langle x\rangle_{\rm IC}$
BHPS1	0.6%	SEA1	0.6%
BHPS2	2.0%	SEA2	1.5%

TABLE I. IC models considered [12].

II. Zc PRODUCTION

We calculate Z_j^c at next-to-leading order (NLO) using the so-called VFNS CT14 next-to-NLO (NNLO) PDF set [17] and the Zj POWHEGBOX matrix element [18], and cross-check our results with aMC@NLO [19]; showering is performed via PYTHIA [20] using the POWHEG [21] and FXFX [22] methods for our baseline and cross-check calculations, respectively. Hadronization is also performed with PYTHIA, while hadrons are decayed via EVTGEN [23] interfaced to PHOTOS [24]. We only consider the decay $Z \to \mu\mu$, and in all cases Z denotes Z/γ^* where $60 < m(\mu\mu) < 120\,\text{GeV}$. More details on our calculations are provided in the Appendix.

The leading-order contribution to Zc production is $gc \to Zc$ as shown in Fig. 1; however, at NLO there are also sizable contributions from $gc \to Zcg$, $gg \to Zc\bar{c}$, $qc \to Zcq$, and $q\bar{q} \to Zc\bar{c}$. The theory uncertainty on Z_j^c is a combination of PDF, factorization and renormalization scale, and strong-coupling (α_s) uncertainties, where the PDF contribution is found to be dominant (since the others largely cancel in the ratio). Charm jets are identified at the particle level by the presence of a long-lived c-hadron with transverse momentum $p_{\rm T} > 2\,\text{GeV}$ produced promptly in the pp collision.

The CT14 global analysis turns on the c and $\bar{c}$ PDFs at $Q = m(c)$, *i.e.* at the charm mass, with initial distributions $c(x, m(c)) = \bar{c}(x, m(c))$ consistent with NNLO matching. At NLO, $c(x, m(c)) = \bar{c}(x, m(c)) = 0$, while at NNLO they are of $\mathcal{O}(\alpha_s^2)$. Additional c content is generated by gluonic radiation for $Q > m(c)$. Following Ref. [12], we consider two categories of non-perturbative IC models: (BHPS) valence-like, inspired by the light-cone picture of nucleon structure [25, 26]; and (SEA) sea-like, where IC $\propto \left[\bar{u}(x, Q_0) + \bar{d}(x, Q_0)\right]$ at an initial scale $Q_0 < m(c)$. In each model, the IC content is considered in addition to the perturbative charm contribution. For each IC category, two values of the mean momentum fraction of the IC PDF at $Q = m(c)$, $\langle x\rangle_{\rm IC} \equiv \int_0^1 x\,\text{IC}(x, m(c))\text{d}x$, are considered: roughly the maximum $\langle x\rangle_{\rm IC}$ value that is consistent with the global PDF analysis of CT14 [17], and a smaller IC contribution (see Tab. I and Fig. 3). Many other IC models exist (see, *e.g.*, Ref. [27]); however, we only consider the BHPS and SEA models as this is sufficient to demonstrate the impact of both low-x and high-x IC.

III. SELECTION AND DETECTOR PERFORMANCE

The LHCb detector is a single-arm spectrometer covering the forward region of $2 < \eta < 5$ [28, 29]. The detector, built to study the decays of hadrons containing b and c quarks, includes a high-precision charged-particle tracking system. The silicon-strip vertex locator (VELO) that surrounds the pp interaction region measures heavy-flavor hadron lifetimes with an uncertainty of about 50 fs [30]. Different types of particles are distinguished using information from two ring-imaging Cherenkov (RICH) detectors, an electromagnetic and hadronic calorimeter system, and a system of muon chambers [31].

Our analysis assumes that the LHCb detector performance will be equivalent in Runs 1 and 2 of the LHC, and that LHCb will collect $5\,\text{fb}^{-1}$ of data at $\sqrt{s} = 13$ TeV in Run 2. For Run 3, we take the detector performance from the LHCb subsystem technical design reports [32–35], and assume $15\,\text{fb}^{-1}$ is collected at $\sqrt{s} = 14$ TeV.

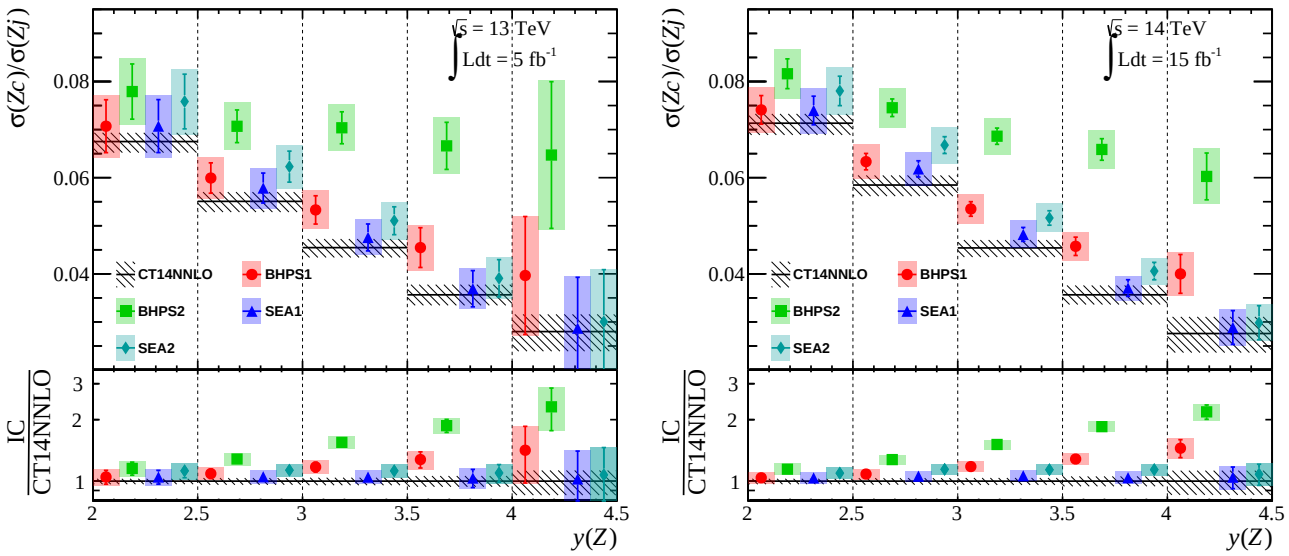

FIG. 4. Predictions for Z_j^c for (left) Run 2 and (right) Run 3. For each IC model prediction, the expected experimental statistical uncertainty is shown by the error bar, while the expected total experimental uncertainty is given by the shaded box. The total theory uncertainty is shown as the hashed box around the CT14NNLO-based prediction. The bottom plots show the relative impact of the various IC PDFs; note the log scale. *N.b.*, the experimental systematic uncertainty is nearly 100% correlated across $y(Z)$ bins; the IC-model predictions are staggered within in each bin to aid readability.

LHCb has demonstrated the ability to make precise measurements of Z boson production [36–38]. Here, we assume only the decay $Z \to \mu\mu$ is used as it provides the most precise experimental measurements. Following Ref. [36], we define the muon fiducial region to be $p_{\rm T}(\mu) > 20\,{\rm GeV}$ and $2 < \eta(\mu) < 4.5$ for Run 2. For Run 3, the $\eta(\mu)$ region is extended to $2 < \eta(\mu) < 5$ due to the improved tracking coverage upstream of the magnet that will be provided by the so-called UT system [34]. Z boson candidates are required to satisfy $60 < m(\mu\mu) < 120\,{\rm GeV}$. Furthermore, we assume that quality criteria are imposed on the track and muon, and take the efficiency of such requirements from Ref. [36].

Jets are clustered using the anti-$k_{\rm T}$ algorithm [39] with $R = 0.5$ as implemented in FastJet [40]. Only visible final-state particles within LHCb acceptance are clustered. As in Refs. [41–43], jets are required to satisfy $p_{\rm T}(j) > 20\,{\rm GeV}$ and $2.2 < \eta(j) < 4.2$ to ensure nearly uniform jet reconstruction and c-jet-identification efficiencies, and only the highest-$p_{\rm T}$ jet in each event is considered (all other jets are ignored). Ref. [42] demonstrates that migration of events in and out of this fiducial region due to detector response has negligible impact on the production ratios studied here; therefore, jet $p_{\rm T}$ resolution effects are not considered in this study. LHCb applies criteria to remove fake jets with a 96% efficiency [44]; we assume these will also be applied in Runs 2 and 3. LHCb discards very high-occupancy events as part of its online data-taking optimization. We again assume that this effect will be the same in the future as it was in Run 1, and reduce the expected signal yields by 10% [44].

A key aspect of the proposed measurement in this article is the ability to efficiently identify (or tag) c-jets. LHCb has demonstrated the ability to identify heavy-flavor-hadron decay vertices in jets with a $\approx 0.3\%$ fake rate [41]. Furthermore, LHCb can determine the c-jet and b-jet yields each with percent-level precision. While we expect the c-jet identification efficiency to improve in future LHCb data taking, here we assume that it is $\epsilon_{\rm tag}(c) \approx 25\%$ as it was in Run 1 [41].

The values of $\epsilon_{\rm tag}(c)$ and $\epsilon_{\rm tag}(b)$ were measured simultaneously by LHCb using heavy-flavor-jet enriched data samples. No assumptions were made about the efficiency values in data, *c.f.* simulation, which led to a high degree of anti-correlation between the $\epsilon_{\rm tag}(c)$ and $\epsilon_{\rm tag}(b)$ measurements; each was assigned a 10% relative uncertainty. Ref. [45] shows that the ratio $\sigma(c\bar{c})/\sigma(b\bar{b})$ is robust with respect to higher-order QCD corrections. Therefore, the ratio $\epsilon_{\rm tag}(c)/\epsilon_{\rm tag}(b)$ can be precisely measured in a data-driven way in an analysis similar to Ref. [46], removing the large anti-correlation effect. In this study, we assume that a 5% relative uncertainty is achieved on $\epsilon_{\rm tag}(c)$ in Runs 2 and 3. Finally, background to Zj events will be at the sub-percent level [44] and approximately cancels in the ratios studied here, so is ignored.

IV. EXPECTED SENSITIVITY

Figure 4 shows the expected distributions and precision on Z_j^c versus the rapidity (y) of the Z for each IC model considered compared to the no-IC prediction. The expected results from the LHCb experiment after Runs 2 and 3 of the LHC are each shown assuming the detec-

tor performs as described above. Most experimental and theoretical uncertainties approximately cancel in this ratio. The dominant contribution to the experimental systematic uncertainty comes from how well $\epsilon_{\rm tag}(c)$ can be measured in data. There will also likely be $\approx 1\%$ contributions from various ratios of effects. These can each be studied using data-driven methods and are not expected to increase the total systematic uncertainty significantly.

From Fig. 4 one can see that valence-like IC has a dramatic impact on Z_j^c at large $y(Z)$, while sea-like IC mostly affects Z_j^c at small $y(Z)$. Both the shape and size of the measured Z_j^c versus $y(Z)$ distribution can be used to study IC(x). By the end of Run 3, we estimate that LHCb will be sensitive to IC of the type found in BHPS models for $\langle x\rangle_{\rm IC} \gtrsim 0.3\%$, and to that found in SEA models for $\langle x\rangle_{\rm IC} \gtrsim 1\%$. The impact of valence-like IC on Z_j^c in the forward region is so large that discovery of IC will be possible already in Run 2 for $\langle x\rangle_{\rm IC} \gtrsim 1\%$. If such a valence-like IC component is observed, then it may even be possible in Run 3 to investigate the c and $\bar{c}$ PDFs separately by tagging the charge of the c-jet. Predictions of Z_j^c in the central region (probed by ATLAS and CMS) are provided in the Appendix. As expected, the impact of valence-like IC is greatly reduced, while sea-like IC affects Z_j^c in a similar way as in forward region.

We conclude our discussion on measuring IC by considering the ratio $\sigma(\gamma c)/\sigma(\gamma j)$, *i.e.* replacing the Z boson with a final-state photon, which would permit probing lower values of Q [47–49]. Such measurements have been made at the Tevatron [50, 51] and are suggestive of IC [52]. The LHCb calorimeter system is not well suited to studying high-energy photons; however, LHCb has demonstrated that it can reconstruct and precisely measure the properties of γ conversions to e^+e^- [53]. It may be possible to measure γc production using converted photons at LHCb [54]. We encourage studying this possibility.

For the large valence-like IC scenario, a sizable intrinsic beauty (IB) component may also be present. While IB is expected to be suppressed relative to IC by a factor of roughly $[m(c)/m(b)]^2$ [55], it may still be possible to observe a large valence-like IB component by studying Zb production. Given that the jet-tagging algorithm developed by LHCb simultaneously determines both the b-jet and c-jet yields, we expect that both Z_j^c and Z_j^b will be measured in the same analysis with about the same precision.

V. IMPACT ON OTHER PROCESSES

The IC content of the proton directly affects the production cross sections of many processes at the LHC. For example, valence-like IC content increases W boson production due to an increased probability for $cs \to W$ scattering [56]. Similarly, the rate at which the hypothetical charged Higgs boson is produced in pp collisions is highly sensitive to IC [57]. Furthermore, an increase

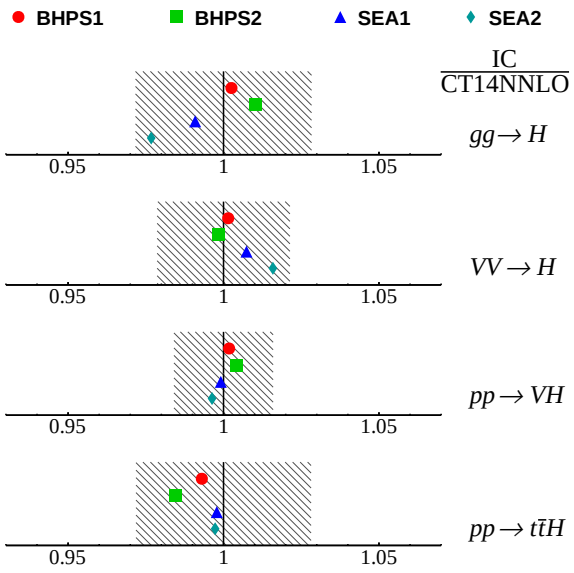

FIG. 5. Impact of IC models on Higgs production in the central region. The hashed boxes show the PDF uncertainties.

in the charm component of the proton must be balanced by a decrease in the other components. This results in IC indirectly affecting many production cross sections via the momentum sum rule.

Figure 5 shows the impact on the major Higgs production cross sections within the acceptance of the ATLAS and CMS detectors, assuming a SM Higgs boson (details on these calculations are provided in the Appendix). Since the PDF uncertainties do not include a contribution due to the assumption of no IC in the proton, one should view the shift due to IC as an additional uncertainty in each Higgs-production process. Higgs production in the central region via gluon fusion ($gg \to H$) is affected by $\lesssim 1\%$ by valence-like IC, but by up to $\approx 2.5\%$ by sea-like IC. Higgs production via vector boson fusion ($VV \to H$) is also affected by sea-like IC by $\approx 2\%$ but in the opposite way. This is expected since adding sea-like IC increases the quark content of the proton while decreasing its gluon content. Associated production of $t\bar{t}H$ is affected by up to 1.5% by valence-like IC due to the large Q, hence large x of one parton, of this gg-initiated process. The predicted sensitivity to IC at LHCb in Run 3 will be sufficient to constrain the effect of valence-like (sea-like) IC on all major Higgs production processes to be $\lesssim 0.5\%(1\%)$. We also note that the presence of IC in the proton could result in diffractive Higgs production [58, 59].

Ref. [60] suggests measuring Hc production as a way of probing the charm Yukawa coupling (Y_c). It is worth noting that the impact of IC on $\sigma(Hc)$ is comparable to that of a SM-like value of Y_c. For both the BHPS2 and SEA2 IC models, $\sigma(Hc)$ with $Y_c = 0$ is about the same as for the no-IC scenario with $Y_c \approx 0.7\,Y_c^{\rm SM}$. Similarly, if $Y_c = Y_c^{\rm SM}$ then these IC models would increase $\sigma(Hc)$ by as much as a $\approx 25\%$ increase in Y_c. Therefore, placing

constraints on IC will be a vital component of determining Y_c using Hc production.

VI. SUMMARY

In summary, measurement of $\sigma(Zc)/\sigma(Zj)$ in pp collisions in the forward region provides a direct probe of a potential intrinsic charm component in the proton wave function. We predict that using data collected in Runs 2 and 3 of the LHC, the LHCb experiment will be sensitive to valence-like IC with $\langle x\rangle_{\rm IC} \gtrsim 0.3\%$, and sea-like IC for $\langle x\rangle_{\rm IC} \gtrsim 1\%$. This sensitivity is sufficient to discover, in the context of a global PDF analysis, the IC predicted by light-cone calculations [25, 26], and to constrain the uncertainty on the affect of IC on Higgs boson production at the LHC to $\lesssim 1\%$. We reiterate that even in the absence of IC, this measurement will provide a useful test of DGLAP evolution for c quarks from low-Q DIS measurements up to the electroweak scale. Finally, a similar analysis of $\sigma(Wc)/\sigma(Wj)$ versus $\eta(\mu)$ can be performed at LHCb to probe the large-x strange PDFs, where the charge of the W boson determines whether the initial parton was an s or $\bar{s}$. Given the large ratio of $\sigma(Wc)/\sigma(Zc)$, precision measurement of the charge asymmetry in Wc production should be possible already in Run 2.

ACKNOWLEDGMENTS

We thank S.J. Brodsky, R. Gauld, P. Koppenburg, W. Melnitchouk, and F. Olness for helpful advice and feedback. P.I. and M.W. are supported by the U.S. National Science Foundation grant PHY-1306550.

APPENDIX

First, we provide some additional technical details about our calculations. The Zj POWHEGBOX calculations are performed in the massless limit for all fermions. In the cross-check calculations performed using aMC@NLO, we consider both massive and massless charm quarks and obtain consistent results to $\approx 1\%$ for Z_j^c in each case with our baseline POWHEGBOX calculations. This agrees with the expectation that threshold effects due to $m(c)$ should be $\mathcal{O}([m(c)/(R\cdot p_{\rm T}(j))]^2) \approx 1\%$; therefore, the dependence of Z_j^c on $m(c)$ is negligible. A $p_{\rm T}$ ordered parton shower is applied using PYTHIA 8, where the leading-order CT14 PDF set is used when calculating the Sudakov form factors for space-like showers. This ensures that for low x and low Q all PDFs remain positive definite, which oftentimes is not the case for NLO and NNLO PDF sets.

The IC PDF sets provided in CT14 are only available at NNLO, while the Zj matrix element used is NLO. The NNLO corrections to Z_j^c are expected to be small [61, 62] (the NNLO corrections to Zj and Zc should largely cancel in the ratio Z_j^c) and covered by the scale uncertainty. As a cross check, we also calculate Z_j^c without IC using CT14 NLO PDFs and find shifts of 1–2% in all but the largest $y(Z)$ bin where the shift is 5%. Each of these is smaller than the PDF uncertainty we assign. We conclude that the mismatch between the order of the IC PDF sets and Zj matrix element has no impact on the conclusions of this study; however, once the LHCb Z_j^c measurement is available, it will be desirable to have Z_j^c calculated at NNLO for inclusion in the global PDF fits.

Since our calculation is performed for the forward region, one could be concerned about threshold effects that may arise when probing the $x \to 1$ region; however, our proposal only involves a differential measurement in $y(Z)$, and so Z_j^c is not sensitive to the $x \to 1$ region. In the five $y(Z)$ bins used in our calculations, the mean values of the lead-parton x are 0.17, 0.21, 0.27, 0.37, and 0.52 in order of increasing $y(Z)$. The fraction of events that involve a parton with $x > 0.7$ is less than 0.5% in all but the largest $y(Z)$ bin where it is 2%. Finally, to check whether the large-x PDF uncertainties are accurate, we calculate Z_j^c using both NLO and NNLO PDF sets from NNPDF [63]. The shifts in Z_j^c are 1–2% in all but the largest $y(Z)$ bin where the shift is 5%; in each $y(Z)$ bin the shift is smaller than the quoted PDF uncertainty.

Figure 6 shows the Z_j^c predictions for the central region. These calculations are performed in the same manner as those for within the LHCb acceptance, but with the muon and jet η requirements changed to $|\eta| < 2.5$. Given the large luminosity that ATLAS and CMS expect to collect, the experimental uncertainty on Z_j^c will be driven by the c-jet tagging. Only the SEA2 model affects Z_j^c by $\gtrsim 10\%$. With enough luminosity – and assuming a c-tagging efficiency of about 10% – it may be possible to improve the sensitivity to valence-like IC in the central region by instead measuring Z_j^c at large $p_{\rm T}(Z)$ [12]; however, we do not expect that equivalent sensitivity to that of LHCb can be achieved by CMS or ATLAS in Run 3. We note that an alternative approach for ATLAS/CMS is proposed in Ref. [64] that involves measuring the ratio ZQ/WQ, where Q denotes all tagged b-jets and c-jets, at large jet $p_{\rm T}$.

For predictions of SM Higgs boson production in the central region, the calculations are performed in the same manner as for Z_j^c; however, only the relative impact of the IC models is provided and only PDF uncertainties are considered. This is sufficient to demonstrate qualitatively how IC affects Higgs production. In all cases we require $|\eta(H)| < 2.5$, along with the following channel-specific requirements: $(VV \to H)$ for vector boson fusion, we require $p_{\rm T}(j) > 20\,{\rm GeV}$, $|\eta(j)| < 5$, and $|\Delta\eta(j)| > 3$; $(pp \to VH)$ for vector boson associated production, we require all leptons from W and Z decays have $p_{\rm T}(\ell) > 20\,{\rm GeV}$ and $|\eta(\ell)| < 2.5$; and $(pp \to t\bar{t}H)$ for top associated production, we require the leptons and b-jets have $|\eta| < 2.5$ and $p_{\rm T} > 20\,{\rm GeV}$.

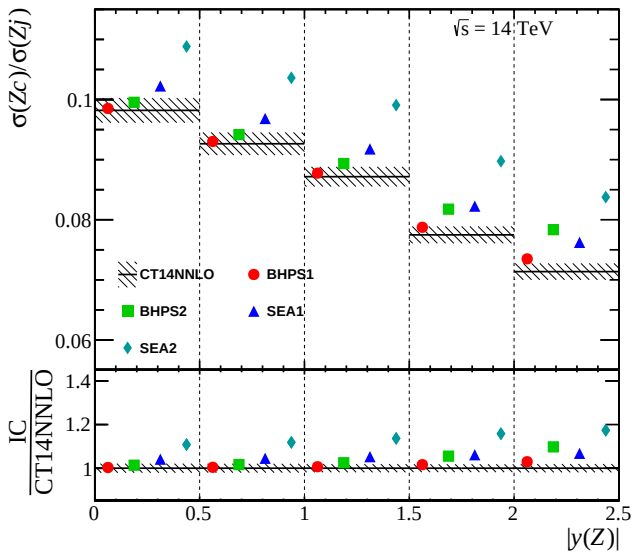

FIG. 6. Predictions of Z_j^c for the central region. No experimental error bars are provided, as these will be driven by the systematic uncertainty on determining the tagged c-jet yield and c-tagging efficiency. Only the SEA2 model affects Z_j^c by $\gtrsim 10\%$. *N.b.*, due to the small effect of IC in the central region, the lower panel here is presented using a linear scale *c.f.* the log scale used in Fig. 4.

[1] S. J. Brodsky, A. Kusina, F. Lyonnet, I. Schienbein, H. Spiesberger, and R. Vogt, Adv. High Energy Phys. **2015**, 231547 (2015), arXiv:1504.06287 [hep-ph].
[2] M. Franz, M. V. Polyakov, and K. Goeke, Phys. Rev. **D62**, 074024 (2000), arXiv:hep-ph/0002240 [hep-ph].
[3] S. Brodsky, G. de Teramond, and M. Karliner, Ann. Rev. Nucl. Part. Sci. **62**, 1 (2012), arXiv:1302.5684 [hep-ph].
[4] M. Gong *et al.* (XQCD), Phys. Rev. **D88**, 014503 (2013), arXiv:1304.1194 [hep-ph].
[5] W. Freeman and D. Toussaint (MILC), Phys. Rev. **D88**, 054503 (2013), arXiv:1204.3866 [hep-lat].
[6] M. G. Aartsen *et al.* (IceCube), Science **342**, 1242856 (2013), arXiv:1311.5238 [astro-ph.HE].
[7] R. Gauld, J. Rojo, L. Rottoli, S. Sarkar, and J. Talbert, (2015), arXiv:1511.06346 [hep-ph].
[8] J. J. Aubert *et al.* (European Muon), Nucl. Phys. **B213**, 31 (1983).
[9] E. Hoffmann and R. Moore, Z. Phys. **C20**, 71 (1983).
[10] B. W. Harris, J. Smith, and R. Vogt, Nucl. Phys. **B461**, 181 (1996), arXiv:hep-ph/9508403 [hep-ph].
[11] F. M. Steffens, W. Melnitchouk, and A. W. Thomas, Eur. Phys. J. **C11**, 673 (1999), arXiv:hep-ph/9903441 [hep-ph].
[12] S. Dulat, T.-J. Hou, J. Gao, J. Huston, J. Pumplin, C. Schmidt, D. Stump, and C. P. Yuan, Phys. Rev. **D89**, 073004 (2014), arXiv:1309.0025 [hep-ph].
[13] P. Jimenez-Delgado, T. J. Hobbs, J. T. Londergan, and W. Melnitchouk, Phys. Rev. Lett. **114**, 082002 (2015), arXiv:1408.1708 [hep-ph].
[14] S. J. Brodsky and S. Gardner, (2015), arXiv:1504.00969 [hep-ph].
[15] P. Jimenez-Delgado, T. J. Hobbs, J. T. Londergan, and W. Melnitchouk, (2015), arXiv:1504.06304 [hep-ph].
[16] Blümlein, Johannes, (2015), 10.1016/j.physletb.2015.12.068, arXiv:1511.00229 [hep-ph].
[17] S. Dulat, T. J. Hou, J. Gao, M. Guzzi, J. Huston, P. Nadolsky, J. Pumplin, C. Schmidt, D. Stump, and C. P. Yuan, (2015), arXiv:1506.07443 [hep-ph].
[18] S. Alioli, P. Nason, C. Oleari, and E. Re, JHEP **01**, 095 (2011), arXiv:1009.5594 [hep-ph].
[19] J. Alwall, R. Frederix, S. Frixione, V. Hirschi, F. Maltoni, O. Mattelaer, H. S. Shao, T. Stelzer, P. Torrielli, and M. Zaro, JHEP **07**, 079 (2014), arXiv:1405.0301 [hep-ph].
[20] T. Sjöstrand, Torbjrn, S. Ask, J.R. Christiansen, R. Corke, N. Desai, P. Ilten, S. Mrenna, S. Prestel, C.O. Rasmussen, and P.Z. Skands, Comput. Phys. Commun. **191**, 159 (2015), arXiv:1410.3012 [hep-ph].
[21] P. Nason, JHEP **11**, 040 (2004), arXiv:hep-ph/0409146 [hep-ph].
[22] R. Frederix and S. Frixione, JHEP **12**, 061 (2012), arXiv:1209.6215 [hep-ph].
[23] D. J. Lange, Nucl. Instrum. Meth. **A462**, 152 (2001).
[24] P. Golonka and Z. Was, Eur.Phys.J. **C45**, 97 (2006), arXiv:hep-ph/0506026 [hep-ph].
[25] S. J. Brodsky, P. Hoyer, C. Peterson, and N. Sakai, Phys. Lett. **B93**, 451 (1980).
[26] S. J. Brodsky, C. Peterson, and N. Sakai, Phys. Rev. **D23**, 2745 (1981).

[27] T. J. Hobbs, J. T. Londergan, and W. Melnitchouk, Phys. Rev. **D89**, 074008 (2014), arXiv:1311.1578 [hep-ph].

[28] A. A. Alves Jr. *et al.* (LHCb collaboration), JINST **3**, S08005 (2008).

[29] R. Aaij *et al.* (LHCb collaboration), Int. J. Mod. Phys. **A30**, 1530022 (2015), arXiv:1412.6352 [hep-ex].

[30] R. Aaij *et al.*, JINST **9**, P09007 (2014), arXiv:1405.7808 [physics.ins-det].

[31] A. A. Alves Jr. *et al.*, JINST **8**, P02022 (2013), arXiv:1211.1346 [physics.ins-det].

[32] "LHCb VELO Upgrade Technical Design Report," (2013), LHCb-TDR-013.

[33] "LHCb PID Upgrade Technical Design Report," (2013), LHCb-TDR-014.

[34] "LHCb Tracker Upgrade Technical Design Report," (2014), LHCb-TDR-015.

[35] "LHCb Trigger and Online Technical Design Report," (2014), LHCb-TDR-016.

[36] R. Aaij *et al.* (LHCb collaboration), JHEP **08**, 039 (2015), arXiv:1505.07024 [hep-ex].

[37] R. Aaij *et al.* (LHCb collaboration), (2015), arXiv:1511.08039 [hep-ex].

[38] R. Aaij *et al.* (LHCb collaboration), JHEP **01**, 064 (2015), arXiv:1411.1264 [hep-ex].

[39] M. Cacciari, G. P. Salam, and G. Soyez, JHEP **04**, 063 (2008), arXiv:0802.1189.

[40] M. Cacciari, G. P. Salam, and G. Soyez, Eur.Phys.J. **C72**, 1896 (2012), arXiv:1111.6097 [hep-ph].

[41] R. Aaij *et al.* (LHCb collaboration), JINST **10**, P06013 (2015), arXiv:1504.07670 [hep-ex].

[42] R. Aaij *et al.* (LHCb collaboration), Phys. Rev. **D92**, 052001 (2015), arXiv:1505.04051 [hep-ex].

[43] R. Aaij *et al.* (LHCb collaboration), Phys. Rev. Lett. **115**, 112001 (2015), arXiv:1506.00903 [hep-ex].

[44] R. Aaij *et al.* (LHCb collaboration), JHEP **01**, 033 (2014), arXiv:1310.8197 [hep-ex].

[45] R. Gauld, U. Haisch, B. D. Pecjak, and E. Re, Phys. Rev. **D92**, 034007 (2015), arXiv:1505.02429 [hep-ph].

[46] R. Aaij *et al.* (LHCb collaboration), Phys. Rev. Lett. **113**, 082003 (2014), arXiv:1406.4789 [hep-ex].

[47] T. P. Stavreva and J. F. Owens, Phys. Rev. **D79**, 054017 (2009), arXiv:0901.3791 [hep-ph].

[48] V. A. Bednyakov, M. A. Demichev, G. I. Lykasov, T. Stavreva, and M. Stockton, Phys. Lett. **B728**, 602 (2014), arXiv:1305.3548 [hep-ph].

[49] S. Rostami, A. Khorramian, A. Aleedaneshvar, and M. Goharipour, (2015), arXiv:1510.08421 [hep-ph].

[50] V. M. Abazov *et al.* (D0), Phys. Lett. **B719**, 354 (2013), arXiv:1210.5033 [hep-ex].

[51] T. Aaltonen *et al.* (CDF), Phys. Rev. Lett. **111**, 042003 (2013), arXiv:1303.6136 [hep-ex].

[52] C. Mesropian and D. Bandurin, Int. J. Mod. Phys. **A30**, 1541002 (2015), arXiv:1409.5639 [hep-ex].

[53] R. Aaij *et al.* (LHCb collaboration), JHEP **10**, 115 (2013), arXiv:1307.4285 [hep-ex].

[54] David Ward, private communication.

[55] F. Lyonnet, A. Kusina, T. Jeo, K. Kovark, F. Olness, I. Schienbein, and J.-Y. Yu, JHEP **07**, 141 (2015), arXiv:1504.05156 [hep-ph].

[56] F. Halzen, Y. S. Jeong, and C. S. Kim, Phys. Rev. **D88**, 073013 (2013), arXiv:1304.0322 [hep-ph].

[57] H. L. Lai, P. M. Nadolsky, J. Pumplin, D. Stump, W. K. Tung, and C. P. Yuan, JHEP **04**, 089 (2007), arXiv:hep-ph/0702268 [hep-ph].

[58] S. J. Brodsky, B. Kopeliovich, I. Schmidt, and J. Soffer, Phys. Rev. **D73**, 113005 (2006), arXiv:hep-ph/0603238 [hep-ph].

[59] S. J. Brodsky, A. S. Goldhaber, B. Z. Kopeliovich, and I. Schmidt, Nucl. Phys. **B807**, 334 (2009), arXiv:0707.4658 [hep-ph].

[60] I. Brivio, F. Goertz, and G. Isidori, Phys. Rev. Lett. **115**, 211801 (2015), arXiv:1507.02916 [hep-ph].

[61] A. Gehrmann-De Ridder, T. Gehrmann, E. W. N. Glover, A. Huss, and T. A. Morgan, in *Proceedings, 12th International Symposium on Radiative Corrections (Radcor 2015) and LoopFest XIV (Radiative Corrections for the LHC and Future Colliders)* (2016) arXiv:1601.04569 [hep-ph].

[62] R. Boughezal, X. Liu, and F. Petriello, (2016), arXiv:1602.08140 [hep-ph].

[63] R. D. Ball *et al.* (NNPDF), JHEP **04**, 040 (2015), arXiv:1410.8849 [hep-ph].

[64] P.-H. Beauchemin, V. A. Bednyakov, G. I. Lykasov, and Yu. Yu. Stepanenko, Phys. Rev. **D92**, 034014 (2015), arXiv:1410.2616 [hep-ph].